

THE TEMPERATURE STRUCTURE OF THE
LOWER ATMOSPHERE.

E.K. Webb

SUMMARY. The mean vertical profile and the small-scale turbulent fluctuations of temperature in the lower atmosphere over flat terrain are discussed for the layer extending to a few tens of metres in height. In general, these have a strong dependence on both the vertical heat flux and the wind speed, as expressed in terms of a stability parameter such as the Richardson number or the ratio of height to Obukhov's length; however, on clear days with moderate winds, the mean temperature gradient up to heights of a few metres over smooth terrain (e.g. grassland) is almost independent of wind speed. In unstable conditions (clear days), the temperature fluctuations are intense, but, at sufficiently large scaled heights, the rising thermal convection plumes are interspersed with sinking air which is entirely devoid of temperature fluctuations, giving short intervals of excellent optical transmission over path lengths of a few metres or perhaps tens of metres. In stable conditions (clear nights), the scaled temperature fluctuation intensity decreases as Richardson number increases up to a critical value, beyond which the temperature exhibits varying behaviour with intermittent quiescence, isolated smooth pulses, waves and turbulence.

1. INTRODUCTION.

Optical refraction in clear air is due to density inhomogeneities, which in turn are almost entirely the result of temperature variations, the effect of humidity variations being relatively minor.

Here we discuss the temperature structure of the atmospheric "surface layer", up to heights of a few tens of metres. Attention is restricted to the ideal case of essentially steady conditions over flat and uniform terrain, for which a fairly detailed knowledge of the structure is now available. The atmosphere is generally turbulent, and we have to distinguish between mean quantities, i.e. averages over a period which may typically be between 5 and 30 minutes, and turbulent fluctuations, ranging in time scale from a small fraction of a second up to a minute or more.

An earlier discussion of atmospheric temperature structure has been given by WEBB (1964). This reference may be consulted for more detail than is given in the present notes.

2. BASIC CONSIDERATIONS.

First, it is necessary to review some basic considerations.

We shall be concerned with the profiles of mean wind speed U and potential temperature θ , as functions height z - in particular, with the gradients $\partial U/\partial z$ and $\partial \theta/\partial z$, which are themselves strongly height-dependent. (Potential temperature differs only a little from actual temperature T , the relationship being close to $\partial \theta/\partial z = \partial T/\partial z + 0.01 \text{ deg. C m}^{-1}$.)⁺

The shearing stress τ (horizontal drag) of the wind is often conveniently represented by the "friction velocity" u_* defined by

$$\tau = \rho u_*^2, \quad \dots(1)$$

where ρ is the mean air density. The shearing stress can be thought of as a downward flux of horizontal momentum. Similarly, the vertical heat flux H may be written

$$H = c_p \rho u_* T_*, \quad \dots(2)$$

where c_p is the specific heat of air at constant pressure, thus defining a temperature scale T_* .

The vertical fluxes are affected by turbulent mixing. There are two points to note. First, in steady conditions the fluxes are essentially constant with height, which means that, on any given occasion, u_* and T_* are constant. Second, u_* and T_* are in magnitude comparable with the actual turbulent fluctuations of velocity components and temperature.

On any given occasion, the atmospheric situation can, in the present context, be completely specified by just two quantities: any one of τ, u_* , or $\partial U/\partial z$, together with any one of H, T_* , or $\partial \theta/\partial z$ (where the gradients $\partial U/\partial z$ and $\partial \theta/\partial z$ are taken at some given fixed reference height).

The origin of temperature variations in the air is, of course, the heating and cooling of the ground by radiation; the air itself is virtually transparent to the radiation. On a clear day, the heated ground produces a lapse of potential temperature ($\partial \theta/\partial z$ negative) and an upward turbulent heat flux (H positive). On a clear night, the ground cools by radiating outwards, producing an inversion ($\partial \theta/\partial z$ positive) and downward heat flux (H negative).

3. THERMAL STABILITY PARAMETER.

When $\partial \theta/\partial z$ is negative (lapse), positive (inversion), or zero, the equilibrium is unstable, stable, or neutral, respectively, in regard to the buoyancy force which will act if an average air sample is displaced vertically. Thus, thermal buoyancy forces tend to enhance the turbulence in the lapse case and suppress it in the inversion case.

⁺ See for example Humphreys, 'Physics of the Air' p. 30, 34. McGraw Hill, 1940 - Ed.

A nondimensional parameter often used to indicate the thermal stability condition is the (height-dependent) Richardson number Ri , which is a measure of the ratio of thermal buoyancy forces to mechanical wind-induced forces. The definition is

$$Ri = \frac{(g/\theta) \partial\theta/\partial z}{(\partial U/\partial z)^2},$$

where g is the acceleration of gravity and θ is the mean absolute temperature. A small value of Ri indicates conditions near to neutral, while a large negative value indicates strong instability and a large positive value indicates strong stability. In this context, "large" refers to a magnitude reaching an appreciable fraction of unity.

In conditions near to neutral, simple "mixing length" theory or dimensional argument shows that the gradients are given by

$$\partial U/\partial z = u_*/kz, \quad \dots(3)$$

$$\partial\theta/\partial z = -T_*/kz, \quad \dots(4)$$

where k is a constant known as von Karman's constant, evaluated experimentally as $k = 0.4$. From Eqs. (3) and (4) it follows immediately that in near-neutral conditions, i.e., for small magnitudes of Ri ,

$$Ri = z/L, \quad \dots(5)$$

where L is Obukhov's length scale defined by

$$L = \frac{-u_*^3}{kgH/c_p\rho\theta}.$$

From Eq. (5) it is evident that at sufficiently small heights, the behaviour is always of the near-neutral type, since Ri is small. With increasing magnitude of Ri or z/L , the effects of buoyancy appear: the mean gradients depart from the z^{-1} relationship, their decrease with height becoming more rapid in the unstable case and less rapid in the stable case; and the relationship of Ri to z/L departs from the exact equality of Eq. (5).

The ratio z/L can be regarded as an alternative form of stability parameter in place of Ri ; all the height-dependent quantities with which we are concerned are, when suitably normalized, universal functions of z/L . Thus, the whole structure of behaviour expands or contracts in height from one occasion to another, in accordance with the magnitude of L .

The strong dependence of L on wind speed is to be noted. It varies approximately as U^3 , since, over terrain of given roughness, u_* is approximately proportional to U . L depends also (inversely) on H , while the values of the other quantities involved are almost invariable. As a guide, over grassland on a clear summer day in middle latitudes $|L|$ is typically around 50 m if the wind strength is 5 m/sec (H is approximately 25 mW cm⁻²). A chart for daytime conditions showing $|L|$ in terms of wind speed and heat flux over different types of surface is given in WEBB (1964).

4. MEAN TEMPERATURE PROFILE.

The temperature profile form is now reasonably well established in the unstable case; in the stable case, an indication of the form is available, but further investigation is needed to set the matter on a firm basis. The detailed forms set out below are those which the writer considers give the best representation.

Unstable (clear day) conditions.

Relevant discussion is to be found in the References (WEBB, 1964; PRIESTLEY, 1959; LUMLEY and PANOFSKY, 1964; WEBB, 1965; DYER, 1967).

Broadly speaking, the profile takes a different form in three different height ranges. In region 1, at the lowest heights, $\partial\theta/\partial z$ follows the z^{-1} dependence of Eq. (4). At height z_m say ($z_m \approx 0.03|L|$), this merges into region 2, where the dependence becomes $\partial\theta/\partial z \propto z^{-4/3}$. Region 3 commences at a height approaching $|L|$: here $\partial\theta/\partial z$ often diminishes abruptly, averaging near zero over periods of several minutes; however, the height at which this occurs varies over periods 5-10 minutes, so that in averages over 15-30 minutes or more the effect is smeared over a range of heights, becoming first apparent at heights around $0.3|L|$.

A complete representation of the profile up to about $0.3|L|$ is as follows, incorporating a smoothing factor effective near height z_m .

$$\frac{\partial\theta}{\partial z} = -\frac{T_*}{kz} \left(1 - \frac{1}{7} \frac{z}{z_m}\right) \quad \text{for } z \leq z_m \quad \dots(6a)$$

(region 1)

$$\frac{\partial\theta}{\partial z} = -\frac{T_* z_m^{1/3}}{k z^{4/3}} \left(1 - \frac{1}{7} \frac{z_m}{z}\right) \quad \text{for } z_m \leq z < 0.3|L| \quad \dots(6b)$$

(region 2)

It should be mentioned that z_m is basically related to a parameter α , the "Monin-Obukhov coefficient", which has significance in studies of region 1. The relationship is

$$\frac{z_m}{L} = 1/7\alpha; \quad \dots(7)$$

from observational data, α is near 4.5, giving $z_m/|L| = 0.0317$.

Over the range covered by these equations, the mean wind profile takes a similar form, leading to the following expressions for Ri.

$$Ri = -\frac{1}{7\alpha} \frac{z}{z_m} \left(1 - \frac{1}{7} \frac{z}{z_m}\right)^{-1} \quad \text{for } z \leq z_m \quad \dots(8a)$$

(region 1)

$$Ri = -\frac{1}{7\alpha} \left(\frac{z}{z_m}\right)^{4/3} \left(1 - \frac{1}{7} \frac{z_m}{z}\right)^{-1} \quad \text{for } z_m \leq z < 0.3|L| \quad \dots(8b)$$

(region 2)

Region 2 covers the Ri range from about 0.03 to 0.6. In this region, Eq. (6b), with the smoothing factor ignored, can be written approximately

$$\frac{\partial \theta}{\partial z} \approx - \left(\frac{H}{c_p \rho} \right)^{2/3} \left(\frac{g}{\theta} \right)^{-1/3} z^{-4/3} \quad \text{for region 2.} \quad \dots(6b\text{-bis})$$

In this equation, u_* is absent, so that in region 2, $\partial\theta/\partial z$ is almost independent of wind speed. On clear days with moderate winds, over a reasonably smooth surface, e.g. grassland, region 2 is generally applicable at heights from less than a metre up to several metres.

Stable (clear night) conditions.

Relevant discussion is to be found in LUMLEY and PANOFSKY, 1964; WEBB, 1965; McVEHIL, 1964.

The following profile forms are applicable; a description of the investigations which led to these is now being completed for publication.

$$\text{For } z/L \leq 1: \quad \frac{\partial \theta}{\partial z} = \frac{-T_*}{kz} \left(1 + \alpha \frac{z}{L} \right) \quad \dots(9a)$$

$$\text{For } z/L \geq 1: \quad \frac{\partial \theta}{\partial z} \approx \frac{-T_*}{kz} (1 + \alpha) \quad \dots(9b)$$

$$\text{For } z/L \leq 1: \quad Ri = \frac{z}{L} \left(1 + \alpha \frac{z}{L} \right)^{-1} \quad \dots(10a)$$

$$\text{For } z/L \geq 1: \quad Ri \approx \frac{z}{L} (1 + \alpha)^{-1} \quad \dots(10b)$$

In this stable case, the value of the Monin-Obukhov coefficient α is close to 5.

The lower region, with $z/L \leq 1$, represents the ordinary turbulent regime in stable conditions. With increasing height in this region, $\partial\theta/\partial z$ passes from the z^{-1} dependence towards a value independent of height, while Ri approaches a limiting value $1/\alpha$. However, at a somewhat lower value, $z/L = 1$ and therefore $Ri = 1/(\alpha+1)$, the next region commences. In this region, there is wide variability, and the profile forms given for $z/L \geq 1$ represent only the approximate average behaviour. It is probable that the upper limit to the above formulation is at $Ri \approx 1$, i.e., from Eq. (10b), $z/L \approx 6$. For Ri larger than 1, the profile forms are indeterminate and widely variable, probably with frequent occurrence of sliding air layers separated by sheets of sharp temperature inversion.

5. TURBULENT FLUCTUATIONS OF TEMPERATURE.

In both unstable and stable cases, the different regions described above are highly significant in respect to the nature of the temperature fluctuations.

Unstable (clear day) conditions. In region 1, which is governed almost entirely by wind-shear turbulence, the temperature fluctuations are of typically random turbulent form.

In region 2, there is a composite interaction of wind-shear and thermal buoyancy effects. As well as the random fluctuations, there are buoyancy-assisted "plumes" which become increasingly prominent at increasing heights; observations show that these are carried along by the wind and tilted over by the wind shear.

In region 3, a striking feature is found. Around the rising warm plumes, the sinking environmental air is often entirely devoid of temperature fluctuations, and a temperature sensor at a fixed point shows temperature-quiescent periods which can range from a few seconds (at heights not much above $0.3 |L|$) up to a minute or more (at heights around $|L|$ and greater).

The temperature-quiescent air provides intervals of excellent optical transmission along paths slanting steeply upwards (30° to 60° to the horizontal) in the downwind direction; this is of the utmost importance in making solar observations (WEBB, 1964; WEBB and COULMAN, 1966). In the case of a near-horizontal line of sight, the benefit of the quiescent air can be enjoyed only if the full length of the optical path lies in this air between the plumes; unfortunately, this means that the path length must be shorter than a few metres if transverse to the wind direction, or a few tens of metres if along the wind direction.

It is emphasized that to encounter the quiescent air the whole optical path must be at sufficient height on the occasion concerned - preferably at least at height $|L|$, and the higher the better. A further point to note is that in the temperature-quiescent air the temperature is almost constant with height, as well as horizontally.

Stable (clear night) conditions. Some optical observations in stable conditions have been reported. (PORTMAN et al, 1962.)

Several investigations have shown that ordinary turbulence of the velocity components dies out when Ri is above a critical value near that mentioned earlier, $Ri = 1/\alpha \approx 0.2$. Temperature fluctuation observations (OKAMOTO and WEBB, in preparation) have shown that the r.m.s. temperature fluctuations, scaled relative to $z \partial\theta/\partial z$, decrease as Ri increases towards about 0.2; when Ri is greater than 0.2, the temperature exhibits varying behaviour, with intermittent quiescence, isolated smooth pulses (usually negative), waves, and turbulence.

Quantitative estimation of temperature fluctuation magnitudes. For rough estimation of u_* : the ratio of u_* to U at height 2 m is $u_*/U_2 \approx 0.05$ over mown lawn (grass height 3 cm),

0.07 - 0.1 over open grassland,

0.12 - 0.16 over a field of cereal of height 1 m.

In middle latitudes, H is around 25 mW cm^{-2} on a clear day, and around -2 to -3 mW cm^{-2} on a clear night.

$$c_p \rho \approx 1.2 \text{ mW sec cm}^{-3} (\text{deg. C})^{-1} \text{ near sea level.}$$

In the following, the units are u_* in cm sec^{-1} , T in deg. C, H in mW cm^{-2} , z in cm.

The magnitude of the temperature fluctuations is given approximately by -

In unstable conditions, region 1: r.m.s. $T \approx 3 T_*$ (11a)

In unstable conditions, region 2: r.m.s. $T \approx 0.15 H^{2/3} z^{-1/3}$ (11b)

In unstable conditions, region 3: amplitude above base temperature $\approx 1.8 T_*$(11c)

In stable conditions, lower region ($z/L < 1$): r.m.s. $T \approx 3 T_*$ (tentative)(12)

The spectrum $F(\kappa)$ of the mean square of T fluctuations, representing the contribution per unit range of wave number κ in radians per unit length, takes the following form for large wave numbers (i.e. scales $1/\kappa$ less than one-tenth of the height z).

$$F(\kappa) = \frac{1}{4} c S \kappa^{-5/3}. \quad \dots(13)$$

The quantities c and S are discussed a little further on.

Also at small scales, the mean-square of the average temperature gradient across a small fixed distance r (aligned in any direction) is given by

$$\text{m.s. of av. temp. grad.} = c S r^{-4/3} \quad \dots(14)$$

This may alternatively be regarded as the mean-square temperature difference between two points distance r apart, divided by r^2 . The quantity c appearing in Eqs. (13) and (14) is a numerical constant, being about 3.

The quantity S depends on the meteorological situation and the height z , being represented approximately as follows -

In unstable conditions, region 1: $S = \frac{(H/c_p \rho)^2}{(kz)^{2/3} u_*^2}$ (15a)

In unstable conditions, region 2: $S = \frac{(0.03 \theta/g)^{2/9} (H/c_p \rho)^{16/9}}{(kz)^{8/9} u_*^{4/3} (1 - Ri)^{1/3}}$ (15b)

In stable conditions,
lower region ($z/L < 1$) $S = \frac{(H/c_p \rho)^2}{(kz)^{2/3} u_*^2} (1-\alpha)^{-2/3} (1-Ri)^{-1/3}$ (16)

In applying these expressions, the following may be noted. θ is absolute temperature, about 300 deg. K. In Eq. (15b), $(1 - Ri)^{1/3}$ is only a little greater than 1 (Ri being negative), and may as well be taken as 1. In any case, the simpler form of Eq. (15a) is not too inaccurate over a fairly large part of region 2. In Eq. (16), it will often be convenient to express Ri in terms of z/L , via Eq. (10a); note that here $(1 - \alpha Ri) = (1 + \alpha z/L)^{-1}$.

The background of the above formulas is given for the unstable case in WEBB (1964) and in the stable case in the paper to be published by OKAMOTO and WEBB.

6. PRACTICAL APPLICATION.

Temperature-quiet patches of air are of frequent occurrence at heights above $|L|$. In these patches, the vertical temperature gradient is almost zero (generally a very slight inversion) in unstable conditions, but is large (a strong inversion) in stable conditions.

From the information reviewed in these notes, we may summarize as follows the best conditions for making optical observations along near-horizontal lines of sight.

To reduce the mean refraction (systematic bending of the optical path) - In general, overcast sky (small $|H|$) with a strong wind (large u_*) is most favourable, as $|T_*|$ is then small. But note that on clear days, at heights up to a few metres over smooth terrain, $\partial\theta/\partial z$ is almost independent of wind strength - cf. Eq. (6b-bis). The line of sight should be at the maximum possible height, to make $|\partial\theta/\partial z|$ as small as possible. In the unstable case, if the optical path is at height greater than $|L|$ and is sufficiently short, the benefit of almost zero $\partial\theta/\partial z$ in the temperature-quiet patches may be encountered for brief intervals.

To reduce the fluctuations of refraction which cause random displacements of optical image -

- (a) For taking advantage of the temperature-quiet patches of air which occur at heights above $|L|$, the best conditions are -
- (i) optical path must be short,
 - (ii) optical path aligned along wind direction, in the unstable case; no comparable information is available for the stable case,
 - (iii) optical path must be as high as possible, generally at least 4m above the ground,
 - (iv) light wind, and smooth terrain upwind,
 - (v) clear sky; if during the day, sun high in the sky,
 - (vi) dry ground over a large area upwind (to keep latent heat of daytime evaporation or, perhaps, nighttime condensation as small as possible, so as not to reduce the magnitude of H).

The aim of (iv), (v), and (vi) above is to make $|L|$ as small as possible.

- (b) If the temperature-quiet patches cannot be used, e.g. if continuous observations are needed, or if the line of sight is too long, or if it is not possible to work at sufficient height above the ground, then the small-scale temperature fluctuations are unavoidable but can be minimized by the following conditions -
- (i) line of sight as high as possible,
 - (ii) strong wind,
 - (iii) heavily clouded sky, and/or near dawn and sunset.
 - (iv) moist ground over a large area upwind.

REFERENCES:

- WEBB, E.K. Daytime thermal fluctuations in the lower atmosphere. Applied Optics, Vol. 3, 1329-1336.
1964
- PRIESTLY, C.H.B. Turbulent Transfer in the Lower Atmosphere. Univ. Chicago Press.
1959
- LUMLEY, J.L. & The Structure of Atmospheric Turbulence. Interscience.
PANOFSKY, H.A.
1964
- WEBB, E.K. Aerial microclimate. Agricultural Meteorology, Met. Monogr.,
1965 Vol. 6, No. 28, 27-58.
- DYER, A.J. The turbulent transport of heat and water vapour in an unstable
1967 atmosphere. Quart. J. Roy. Meteorol. Soc., Vol. 93, 501-508.
- McVEHIL, G.E. Wind and temperature profiles near the ground in stable
1964 stratification. Quart. J. Roy. Meteorol. Soc., Vol. 90,
136-146.
- WEBB, E.K. & Daytime seeing and thermal structure in the lower atmosphere.
COULMAN, C.E. Nature, Vol. 212, 58-59.
1966
- PORTMAN, D.J. Some optical properties of turbulence in stratified flow near
ELDER, F.C. the ground. J. Geophys. Res., Vol 67, 3223-3235.
RYZNAR, E. &
NOBLE, V.E.
1962
- OKAMOTO & In preparation.
WEBB, E.K.

THE ATMOSPHERE AS AN OPTICAL
TRANSMISSION MEDIUM.

C.E. Coulman

SUMMARY. The influence of the atmosphere on the transmission of optical radiation is briefly reviewed and one aspect, namely scattering by refractive inhomogeneity, is dealt with in detail. Geodetic and astronomical observations are often hampered by blurred, unsteady, scintillating images transmitted through the atmosphere. Existing theories of wave propagation in non-uniform media are reviewed and recent methods of measuring fluctuations of the intensity and phase of a wave and of the quality of an optical image are described. It is shown that optical image quality can be predicted from measurements of the fluctuating atmospheric temperature field in a wide range of circumstances of practical interest.

1. INTRODUCTION.

The title of this paper covers so broad a field that we shall sketch the outline of the subject in the briefest detail and quickly narrow the discussion down to review a particular topic which is especially relevant to optical measurements in geodesy.

The transmittance of the Earth's atmosphere for optical radiation is shown, as a function of wavelength λ , in Fig. 2.1. We restrict interest now to the region $0.4 < \lambda < 1.0 \mu\text{m}$, in which transmittance is a smoothly varying function of λ on account of the absence of strong absorption bands. The attenuation of radiation by the constituents of a clear atmosphere is often augmented by the absorbing and large-angle scattering effects of fogs and clouds. Such effects vary widely with time and location but often limit the range of optical propagation.

Optical radiation is also scattered in a transparent medium if its refractive index is non-uniform. The Earth's atmosphere is generally refractively inhomogeneous in space and time; the scale of this inhomogeneity is large compared with the wavelength of light and therefore causes small angle, or forward, scattering. It is with this aspect of the atmospheric transmission of light that we shall deal in detail, in order to show that atmospheric "seeing" may be studied quantitatively to yield results of practical value in observational sciences such as geodesy and astronomy.

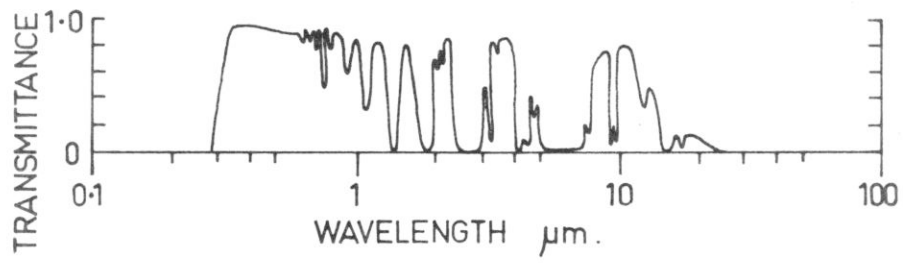


FIG: 2.1

Atmospheric transmittance as a function of wavelength λ .

2. OPTICAL PROPAGATION IN THE ATMOSPHERE.

Because the refractive index of the atmosphere varies systematically with altitude, light traverses a curved path through the air and there is generally a difference between the true and apparent directions in which an object is seen. A correction for this "atmospheric refraction" is usually made in geodetic and astronomical observations. In addition to this regular component of variation, the random variations of refractive index cause fluctuations in the quality of optical images propagated through the atmosphere which often limit the precision of measurements made along both horizontal and slanting lines of sight.

The refractive-index of the atmosphere fluctuates in time and space and causes amplitude and phase fluctuations of a wave as it propagates. Consequently, an image formed by focussing such a wave usually exhibits fluctuations in INTENSITY, SHARPNESS and POSITION. These effects we call SCINTILLATION, IMAGE BLURRING and IMAGE MOVEMENT respectively; the term "SEEING" is given to the overall phenomenon. There seems to be no general agreement on terminology as yet, but these terms will be used consistently throughout this paper.

A theory of the propagation of a plane wave in a locally homogeneous isotropic, turbulent medium has been given by TATARSKI, 1959. The spatial statistics of amplitude and phase fluctuations of such a wave may be described by the structure function $D_A(r)$ of the logarithm of the amplitude, and the phase structure function $D_S(r)$. A structure function is a statistical second moment defined, in one dimension and for a property S , by

$$D_S(r) = \left\langle [S(x) - S(x+r)]^2 \right\rangle, \quad \dots (1)$$

where r is a span along coordinate x and the sharp brackets denote the averaging operation. For a large range of scale sizes (r -values), called the "inertial sub-range", Kolmogorov has demonstrated (KOLMOGOROV, 1941) that the structure function of a conservative, passive variable, such as refractive index n , may be expressed in terms of the correlation parameter r as

$$D_n(r) = C_n^2 r^{2/3} \quad \dots (2)$$

For a propagation path of length x_1 , Tatarski has shown that

$$D_A(r) + D_S(r) = 2.91 \left(\frac{2\pi}{\lambda}\right)^2 r^{5/3} \int_0^{x_1} C_n^2(x) dx, \quad \dots (3)$$

where C_n is the refractive-index structure coefficient (TATARSKI, 1959). The sum $D_A(r) + D_S(r)$, denoted by $D_W(r)$, is usually called the wave structure function. For light from a celestial source propagating through the Earth's atmosphere, we may rewrite Eq. (3) as

$$D_W(r) = 2.91 \left(\frac{2\pi}{\lambda}\right)^2 r^{5/3} \sec^2 \omega \int_{z_T}^{z_m} C_n^2(z) dz, \quad \dots (4)$$

where z is the vertical coordinate with origin at the ground, ω is the angle between zenith and the viewing direction, and we neglect effects due to curvature of the Earth. An image is assumed to be formed by a diffraction-limited, axially symmetric optical system situated at height z_T , and z_m is the height above which the value of C_n becomes negligibly small.

Although it is quite practicable to measure these structure functions it is often more convenient to specify quality in a way more directly related to readily observable features of an image. A suitable property is the Optical Transfer Function (OTF).

The modulus of the complex OTF is a measure of the contrast reduction suffered by each Fourier component (spatial frequency) of the object after transmission through the entire imaging system. Fluctuations in the argument of the OTF indicate changes in the position and symmetry of the point-image in the focal plane. We thus have a precisely definable measure of image blurring and image movement. See, for a full treatment, BORN and WOLF, 1959 and, for a good descriptive treatment, PERRIN, 1960.

The theory which yields Eq. (3) and (4) involves approximate solutions of the wave-equation whose range of validity is currently being questioned. However, without involving such methods, the modulus of OTF, or modulation transfer function (MTF), $\langle M(f) \rangle_{t'}$, for an image averaged over a long time, $t' \rightarrow \infty$ may be written:

$$\langle M(f) \rangle_{t' \rightarrow \infty} = A(f) \exp [-\frac{1}{2} D_w(r)] \quad \dots (5)$$

The spatial frequency f in the image plane is related to r in the entrance-pupil plane by

$$f = \frac{r}{\lambda F} , \quad \dots (6)$$

where F is the focal length of the imaging system. When $D_w(r) = 0$, as in a uniform medium where $C_n = 0$.

$$\langle M(f) \rangle_{t'} = A(f), \quad \dots (7)$$

and $A(f)$ represents the time-independent MTF of the imaging instrument.

3. THE MEASUREMENT OF "SEEING" EFFECTS.

The measurement of "seeing" is important to check the validity of theories which have been developed, to ascertain limits on the precision of optical observations under any given conditions and to aid the optimal design of instruments and the selection of sites for such observations. We shall consider measurements of:-

- (1) Intensity fluctuations
- (2) Phase fluctuations
- (3) Optical Transfer Function

The statistics of intensity fluctuations of the wavefield may be readily investigated by means of two photo-detectors spaced a distance r apart. TATARSKI and others measured the mean-square fluctuation, the correlation function and structure function of intensity for light transmitted along horizontal paths over level land (TATARSKI, 1959). For propagation distances less than about 500 m the early theoretical work of Tatarski was confirmed by such measurements. However, in conditions which yield strong intensity fluctuations and for distances exceeding 500 m Gracheva and Gurvich discovered serious discrepancies between their later measurements and the theory (GRACHEVA and GURVICH, 1965). Although attempts have been made to reconcile these differences it is generally felt that present theoretical treatments are still not adequate to account for all the observed properties of a fluctuating wave-field. However, as mentioned above, some information on image quality can be obtained without invoking the approximations involved in Tatarski's theory.

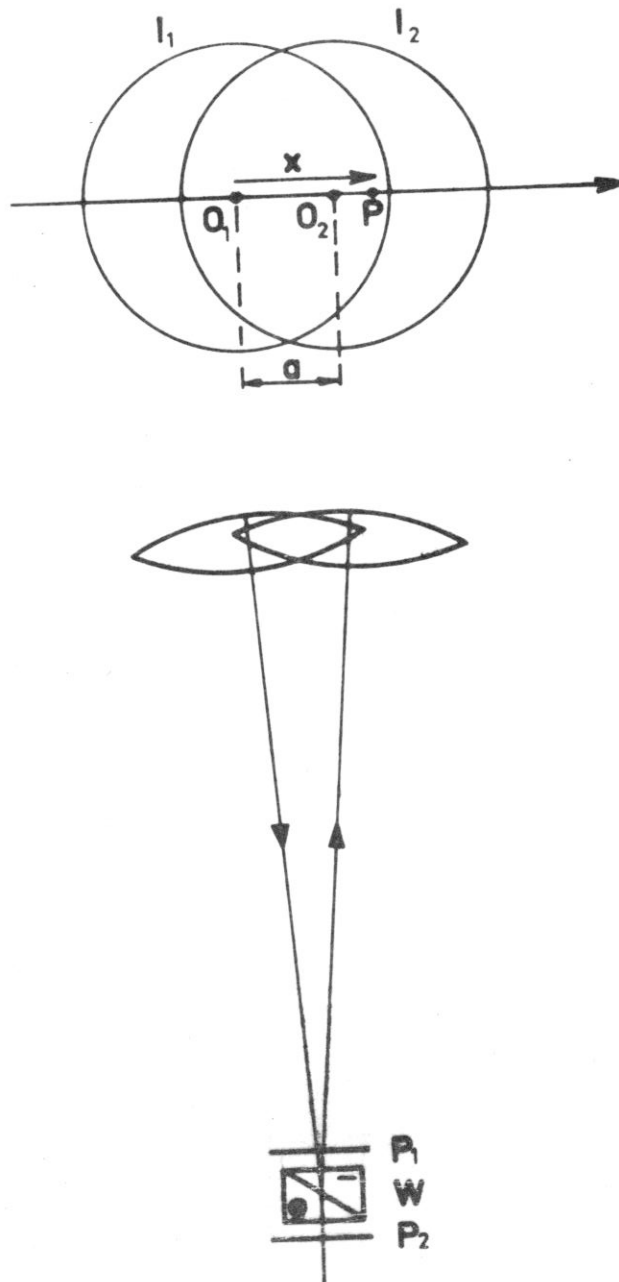


FIG. 2.2

A Wollaston prism W and polarizers P_1 , P_2 are used to form two sheared images of a lens. The upper diagram shows the axial view to a larger scale.

Few attempts have been made to measure the phase fluctuations of a wave directly, but Coulman has recently described an instrument to measure the phase structure function (COULMAN, 1967). For this we require an interferometer in which fluctuations of the fringe pattern are proportional to the phase difference between points on the wavefront distant r apart. The wave-shearing interferometer is just such a device. (BATES, 1947). In a shearing interferometer the wavefront to be studied is caused to interfere with a displaced image of itself; the optical system of the interferometer is therefore essentially an image doubling system. A compact device which splits one beam of light into two beams inclined at an angle to each other is a Wollaston prism made from birefringent material, e.g. quartz or calcite (FRANCON, 1966). If this is placed at the focus of a lens, with appropriately oriented polarizers, two images of the lens aperture displaced relative to each other will be seen. If the wavefront converging to a focus is perfectly spherical the fringe pattern in the overlap region of images I_1, I_2 (Fig. 2.2) will not depend on the shear. When the wavefront is deformed, the fringe shift, or change of order of interference Δm , at a point x from the origin will be

$$\Delta m = \frac{1}{2\pi} [S(x) - S(x - a)] , \quad \dots (8)$$

for linear shear a .

Thus all we have to do is measure the amount by which a fringe shifts to determine the phase difference $[S(x) - S(x - a)]$ and the linear shear takes the place of the correlation parameter r . This is the scale size at which we are examining the phase field. With the dynamic version of this instrument which has been built phase fluctuations which occur at frequencies up to 50 Hz may be measured to $\lambda/100$.

Some photographic measurements of MTF associated with atmospheric image transmission have been made (ROGERS, 1965) but dynamic measurements, utilizing a point-image analyser, have been more rewarding (COULMAN, 1965; 1966). With this instrument the modulus and argument of the OTF of a system comprising an image-forming instrument and an atmospheric propagation path may be continuously recorded.

The dependence of image quality and stability (as measured by the OTF) on range and micro-meteorological conditions has been investigated for a horizontal path over level land (COULMAN, 1965; 1966) empirical relationships have been deduced to enable the MTF and root-mean-square angular image movement $\langle (\Delta\alpha)^2 \rangle^{1/2}$ to be calculated from measurements of the atmospheric temperature structure function $D_T(r)$. These experiments substantially confirm the theory discussed in Section 2, and a modified theory for spherical waves, and therefore lead to the important result that image quality may be predicted from information about the fluctuating atmospheric temperature field (FRIED, 1966).

4. THE PREDICTION OF "SEEING" QUALITY.

Measurements of air-temperature fluctuations and wind speed are often cheaper and easier to make than are optical measurements involving well-aligned, rigidly-mounted instruments. Direct measurements of C_n in the atmosphere are also difficult but at optical wavelengths refractive index fluctuations are almost linearly related to temperature fluctuations; thus

$$C_n \approx \frac{8 \times 10^{-6} p C_T}{a^2} , \quad \dots (9)$$

where θ is absolute temperature in $^{\circ}\text{K}$, p is pressure in millibars and C_T is the temperature structure coefficient. Hence, with the above-mentioned experiments as justification we may re-write Eq. (3) and (4), which define the wave structure function, in terms of C_T .

Direct measurements of C_T as a function of altitude are available from two sources; Koprov & Tsvang have made measurements at several heights up to 4 km with an instrumented aircraft (KOPROV and TSVANG, 1966) and Coulman has investigated the lowest 200 m of air in detail with captive-balloon-borne equipment. (COULMAN, 1969). Indirect estimates of C_T for greater altitudes have been made (HUFNAGEL, 1966). These results have been compiled in Fig. 2.3 to yield the best available estimates of the C_T^2 - profile for some broad classes of daytime conditions.

Let us examine a few examples of the use of these results to calculate the optical performance of, say, an 11 cm diameter lens in some typical atmospheric conditions. In a typical surveying application we might consider viewing an object along a horizontal line of sight 0.5 km long at a height of 2 m above level grassland. Taking a typical midday value of C_T^2 from Curve (1), Fig. 2.3, we obtain the long-time-averaged MTF shown by the full line in Fig. 2.4; the broken line represents $A(f')$ the MTF of the lens in a "perfect" atmosphere. In the late afternoon conditions, Curve (2) Fig. 2.3, we obtain the dash-dot line for the MTF in Fig 2.4

Spatial frequency f' is expressed in cycles per unit angle of field to render the results independent of focal length F of the imaging system.

$$f' = Ff. \quad \dots (10)$$

This is common practice in optics; the resolution cut-off limit of an instrument is customarily quoted in arc sec. The r.m.s. image movement for this example is:-

$$\langle (\Delta\alpha)^2 \rangle^{1/2} = 2.8 \text{ arc sec (midday)}$$

$$\langle (\Delta\alpha)^2 \rangle^{1/2} = 0.44 \text{ arc sec (afternoon)}$$

In geodetic applications where an extra-terrestrial object (e.g. a retro-reflecting satellite) is viewed we must consider propagation through the entire atmosphere whose C_T^2 -profile, typical of clear midday summer conditions, is given by Curve (1), Fig. 2.3. We utilize Equations (4), (5) and (9), with $\sec \omega = 1$ for zenith viewing, to calculate the MTF, $\langle M(f') \rangle_{t, \infty}$ of the system: atmosphere plus 11 cm lens. The results are shown (Fig. 2.5) for four values of z_T , the height above ground at which the lens is mounted, to illustrate the improvement in image quality obtainable by raising a telescope above ground level by means of a tower. The values of $\langle (\Delta\alpha)^2 \rangle^{1/2}$ corresponding to the four cases considered are given below.

$\langle (\Delta\alpha)^2 \rangle^{1/2}$ arc sec	Observation height z_T metres
0.95	2
0.84	10
0.64	30
0.45	100

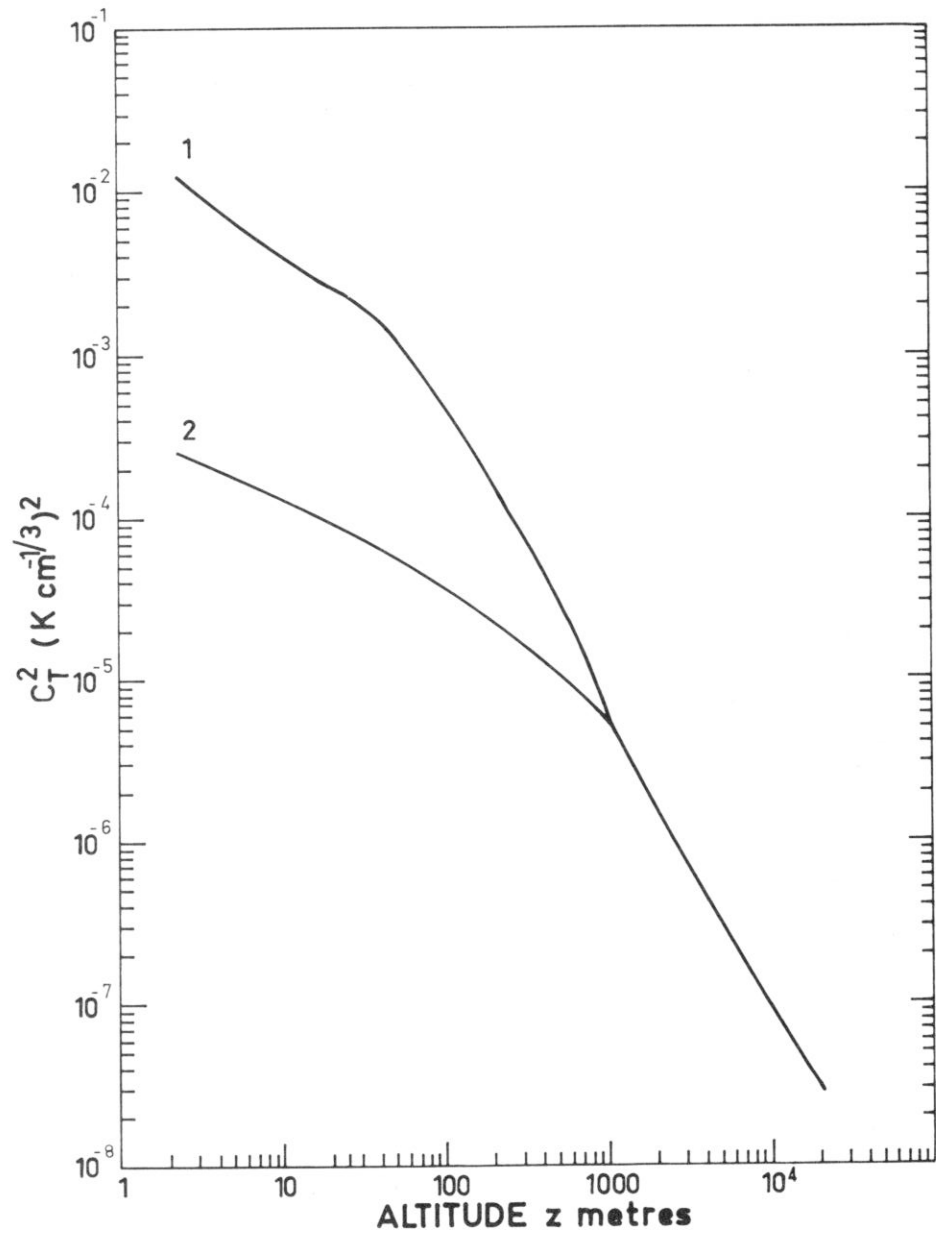


FIG: 2.3

Atmospheric temperature structure coefficient C_T varies with altitude and time of day. C_T^2 is plotted against z , (1) for typical midday conditions and (2) for late afternoon conditions.

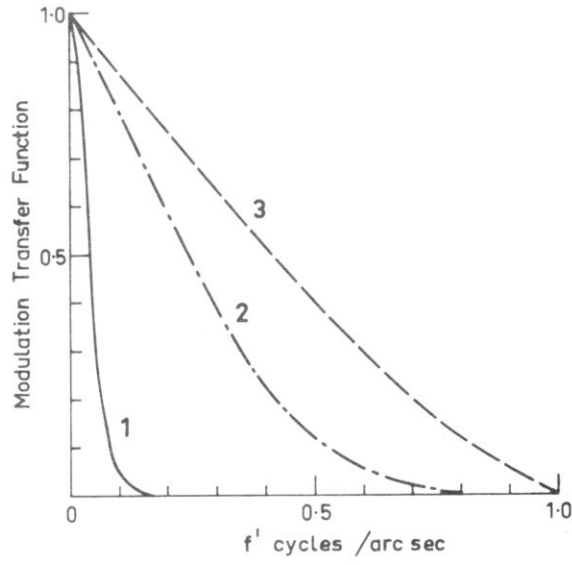


FIG: 2.4

MTF for 11cm diameter lens viewing point source along horizontal path 0.5km long at 2m height. (1) Midday conditions, (2) late afternoon conditions (3) lens in uniform atmosphere. $\lambda = 0.55 \mu\text{m}$.

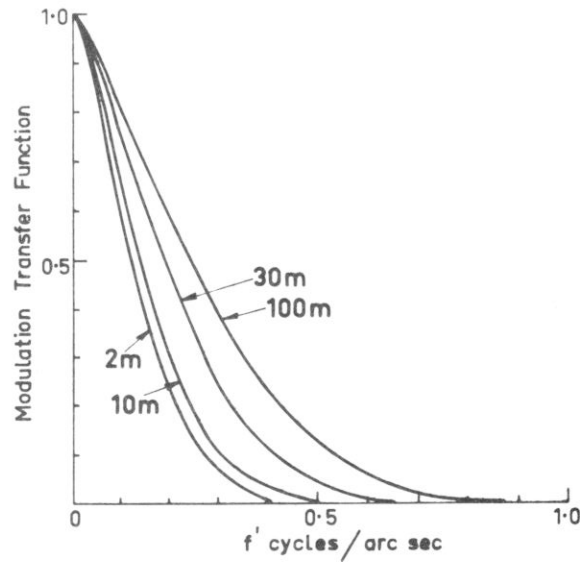


FIG: 2.5

MTF for 11cm diameter lens viewing zenith through average midday atmosphere. Four values of lens height above ground, z_T in metres are shown $\lambda = 0.55 \mu\text{m}$.

Further improvements in performance are obtainable by the use of very short image-averaging times (i.e. short exposures) and by selection of especially favourable intervals of good "seeing" which occur in daytime in consequence of convective thermal structure in the lower troposphere. These matters are dealt with in detail in COULMAN, 1969.

5. THE FUTURE.

In principle there seems to be no reason why the approach outlined should not be used in all circumstances of interest to optical observers. However, further research is necessary before this can be achieved in practice. Far more measurements of C_T as a function of altitude and general meteorological conditions are required and of major importance is the extension of present theoretical and experimental treatments to atmospheric conditions which do not approximate locally homogeneous, isotropic turbulence. Such conditions often exist at night and early in the morning.

REFERENCES.

- TATARSKI, V.I. Wave Propagation in a Turbulent Medium. Translated R.Silverman
1959 1961. McGraw Hill, New York.
- KOLMOGOROV, A.N. Dok. Akad. Nauk SSSR. Vol. 30, No. 301. Translated 1961 Turbulence,
1941 ed. Friedlander, S.K. and Topper, L. Interscience Pub., New York.
- BORN, M and WOLF, E. Principles of Optics. Pergamon Press Inc., New York.
1959
- PERRIN, F.H. J. Soc. Mot. Pict. & Tele. Engrs. Vol. 69, No. 239
1960
- HUFNAGEL, R.E. and STANLEY, N.R. J. Opt. Soc. Am. Vol. 54, No. 52.
1964
- GRACHEVA, M.E. and GURVICH, A.S. Izv. V.U.Z. Radiofiz. Vol. 8, No. 717.
1965
- COULMAN, C.E. Proc. Astron. Soc. Australia. Vol. 1, No. 67.
1967
- BATES, W.J. Proc. Phys. Soc. Vol. 59, No. 940.
1947
- FRANCON, M. Optical Interferometry, Academic Press, New York.
1966
- ROGERS, C.B. J. Opt. Soc. Am., Vol. 55, No. 1151.
1965
- COULMAN, C.E. J. Opt. Soc. Am., Vol. 55, No. 806.
1965
- COULMAN, C.E. J. Opt. Soc. Am., Vol. 56, No. 1232
1966
- FRIED, D.L. J. Opt. Soc. Am., Vol. 56, No. 1372
1966
- KOPROV, V.M. and TSVANG, L.R. Izv. Atmos. i Okean. Fiz., Vol 2, No. 1142.
1966
- COULMAN, C.E. Solar Phys. (In Press).
1969
- HUFNAGEL, R.E. Restoration of Atmospherically Degraded Images, Woods Hole
1966 Summer Study, Washington, D.C.

DISCUSSION: PAPERS 1 and 2.

Chairman: Professor P.V. Angus-Leppan.

WEBB: Atmospheric temperature structure

COULMAN: Optical transmission.

OWENS: How is the Richardson number Ri determined?

WEBB: By determining the wind velocity and measuring the temperature. Obukhov's length L is the most significant parameter in determining Ri .

KIRSCH: What instrument is used to measure temperature and is the measurement recorded an instantaneous temperature?

WEBB: Sensing elements with significant lag are to be preferred so as to eliminate some of the short-period fluctuations. In dealing with the temperature profile it should be noted that although temperatures fluctuate widely, the temperature difference between points at different elevations is a less variable quantity. Thermistors, quartz crystal thermometers or thermocouples can be used to measure temperature.

ANGUS-LEPPAN: The lens of aperture 11 cms. is chosen as an example by Coulman because it is stated to be the diameter appropriate to an accuracy of 1 sec. Yet the telescope of a 1 sec. theodolite is closer to 4 cms. than 11 cms.

COULMAN: A diameter of approximately 11 cms. is necessary to resolve two points which are one second apart. Setting a crosshair onto a particular feature to an accuracy of 1 sec. does not require a resolution of 1 sec., as the centre can be estimated to an accuracy well beyond the resolution.

OWENS: Do scaling parameters retain their relevance under conditions of turbulence?

WEBB: Yes. The fundamental quality is flux - of heat or momentum or other properties - and turbulence is merely a manifestation of flux.

McQUISTAN: In determining C_T you require temperature. What is the time lag in your temperature measurements, and what is the relationship between this lag and the measurements of phase structure function? What are the frequencies of fluctuation?

COULMAN: The temperature apparatus provides a mean over two minutes, which is sufficiently long to damp out the short-term fluctuations. Temperature structure function is given by:

$$D_T(t) = \langle [T(x) - T(x+t)]^2 \rangle$$

(t is an interval, x a point in time and T represents temperature).

Our instruments are capable of recording frequencies of up to 50 cps. In the atmosphere there are fluctuations at 30 - 40 cps though above 30 cps there is not much 'power'.

A REVIEW OF ATMOSPHERIC DISPERSION MEASUREMENTS
IN GEODESY AND METEOROLOGY

James C. Owens

SUMMARY. Single-wavelength or broadband optical methods of distance and horizontal angle measurement are capable of accuracies as high as a few parts per million under good conditions. The two-wavelength and three-wavelength dispersion methods now under development make possible improvements of one and two orders of magnitude, respectively, in distance measurement, and permit the determination of average water vapor density along a line to an accuracy of 0.5%. The dispersion method could also be applied to angle measurement, but this problem appears considerably more difficult and an accuracy of one or a few seconds of arc is probably the best that will be attainable.

1. INTRODUCTION.

Techniques of geodetic measurement have improved dramatically within the last few years. Details may be found in a comprehensive recent book (JORDAN-EGGERT-KNEISSL, 1966), in an excellent survey paper (BENDER, 1967), and in the collections of papers presented at two recent conferences (IAG, 1965; IAG, 1967). Here we briefly review the most promising of the methods for reducing the atmospheric uncertainties in geodetic measurement, the use of atmospheric dispersion, and describe its application to distance, angle, and water vapor measurement. Additional details of recent work on distance measurement by the dispersion method and other techniques can be found elsewhere (OWENS, 1968).

2. DISTANCE MEASUREMENT.

Outline of Method. The most convenient technique for geodetic measurement consists of measuring the transit time of electromagnetic waves over the path, multiplying this transit time by the propagation velocity of the radiation in vacuum, and applying an appropriate correction for the refractive index of the atmosphere along the path. Because pulse techniques do not provide the requisite precision at present and direct optical interferometry is precluded by atmospheric turbulence, the transit time is normally found through measurements of the phase of a radio-frequency signal. To provide directivity, this signal is usually transmitted as modulation on a micro-wave or optical carrier wave.

The principal limitation to the accuracy of these measurements is the uncertainty in the average refractive index over the path resulting from inhomogeneity and turbulence in the lower atmosphere. The average refractive index is ordinarily estimated from measurements of pressure, temperature, and humidity made at one or more points along the path. Under favorable circumstances, when the meteorological conditions along the path are uniform, distance measurements reproducible to one or two parts per million (ppm) can be obtained. More commonly, however, reproducibilities of several ppm or more are observed, and systematic errors of several ppm are found during network adjustments. Although these limitations apply to both optical and microwave systems, the much smaller effect of water vapor on the optical refractive index (only about 1% of the effect in the microwave region) should permit the corrections to be made with somewhat higher accuracy in optical than in microwave measurements.

A direct optical method for determining the desired average refractive index to higher accuracy has been repeatedly suggested, although its technical feasibility has not been clear until recently. A brief history of the idea is given elsewhere (OWENS, 1968). The method is based on the fact that the refractive index n of the lower atmosphere is dispersive in the visible spectral region, and hence two light signals traversing the same path but having different wavelengths will travel at slightly different velocities (OWENS, 1967). Because $(n - 1)$ at a given vacuum wavelength is proportional to air density for dry air, the difference in refractive index, and hence the difference in transit time for the two signals, will be proportional to the average air density over the path. A measurement of the difference in transit times, therefore, can be used to give the average density over the path. From this quantity the average refractive index for either wavelength may be calculated, providing the desired correction for the distance measurement.

The refractive index of air increases more strongly than linearly as the wavelength is reduced, and hence the shorter of the two wavelengths should be chosen in the violet or near ultraviolet spectral region in order to provide a large dispersion. The longer wavelength is less critical, but should be in the red or near-infrared region. The atmosphere increases the transit time for all wavelengths by about 300 ppm at sea level over the time which would be required in vacuum. The difference in transit time for 6328 Å and 3660 Å, a suitable pair, is about 30 ppm, giving a difference in apparent path length of about 40 cm on a 15-km path. If the difference is measured to one part in 300 (to 1.3 mm in this example), the average atmospheric density can be determined to approximately the same fractional precision, and hence the true distance to about $(1/300)(300 \text{ ppm}) = 1 \text{ ppm}$. By thus providing rapid and accurate spatial averaging of refractive index, the dispersion method should reduce significantly the present limitations to the accuracy of long-range distance measurement.

Expected Accuracy. Three types of errors must be considered: (1) instrumental, (2) dispersion, and (3) geometrical. The first type consists of such errors as uncertainties in the optical wavelengths, in the modulation frequency, and in the effective modulation point. The second type consists of errors due to inadequate knowledge of the dispersion parameters which are required in the calculation of the average refractive index from the measured dispersion. This is primarily a problem of variations in air composition. The data required to estimate this error has been given in a recent review of refractive index formulas (OWENS, 1967), and the analysis in humidity. It can be shown that an error of 9 mb in the average partial pressure of water vapor assumed (which corresponds to a relative humidity of about 50% at 15°C.) leads to an error of 1 ppm in the length determination. For most purposes, therefore, a rough estimate of the average humidity will suffice.

The third type of error is due to refraction and the resultant curvature and noncoincidence of the ray paths for the different wavelengths. A thorough analysis of these effects has been given by THAYER (1967), who found that the errors were very small except for very long paths and unusual refractive conditions and could be made negligible by assuming a standard refractive index gradient. For a 25-km path and a typical optical refractive index gradient, -30 ppm/km, the entire correction is only 3×10^{-8} of the distance. For ground-to-ground paths, none of the geometrical effects are as important as a 5% uncertainty in relative humidity, which seems to be about the minimum that can be achieved when humidity is measured at both ends of the path. (THAYER, 1967). Thayer concluded that the dual wavelength optical method could provide an accuracy of about 0.1 ppm except for paths more than 25 km long or in tropical weather conditions of high humidity and temperatures above 25°C . Similar conclusions have been reached by McQUISTAN (1968).

In the same report, Thayer considered a three-wavelength system, utilizing measurements at a wavelength of 3 cm in addition to 6328 \AA and 3660 \AA . The large microwave-optical dispersion due to water vapor would give an accurate measurement of the average water vapor density over the path. Such a three-wavelength system should be capable of accuracies as high as 0.02 or 0.03 ppm for distances up to 50 km and temperatures up to 30°C under reasonably normal refractive conditions.

The vacuum velocity of light, c , is not known exactly, but this uncertainty is not a source of error in the same sense as those listed above. No triangle non-closures, for example, will result from this uncertainty; its only effect is that there may be a general scale correction factor which should be applied to the entire geodetic network. Because no non-electromagnetic method of distance measurement accurate to 0.1 ppm or better is available, this scale factor will remain unknown until the velocity c is determined to higher accuracy.

Instruments and Results. Several groups have been, or are now, working on dispersion instruments. Fowler and Castellano used lasers having the wavelengths 6328 \AA and $1.15 \mu\text{m}$, finding that the corrected length of a 17.5-km line could be measured with a precision of about 3 ppm (FOWLER and CASTELLANO, 1966). They are now building an improved instrument using lasers at 4880 \AA and 6328 \AA . Thompson and Wood have used a modified Geodimeter to measure the dispersion of air with four spectral lines of mercury between 4048 \AA and 5790 \AA and path lengths of 7.5 and 15 km (THOMPSON and WOOD, 1965). They have found it difficult, however, to modify this commercial instrument for fully satisfactory operation. Finally, Sullivan has used measurements of dispersion in the microwave region to determine average water vapor and dry air densities (SULLIVAN, 1965). By taking measurements at 15.6 and 31.2 GHz, on either side of the 22-GHz water vapor line, and at 45 and 90 GHz, bracketing the several oxygen lines near 60 GHz, he was able to reduce the rms fluctuation of distance measurements made with a 10-GHz instrument over a 23-km path from 13 ppm to about 2 ppm.

The most successful instrument, apparently, has been the one developed in the Wave Propagation Laboratory of the ESSA Research Laboratories in Boulder, Colorado. A block diagram of this instrument is shown in Fig. 3.1. Details of instrument design and operation are available elsewhere (OWENS, 1968; EARNSHAW and OWENS, 1967). For light of either wavelength passing out and back through the modulator, the intensity at the appropriate detector, averaged over a time long in comparison with the modulation period, will be a maximum if the round-trip transit time is an integral multiple of the modulation period. By observing this intensity, one can measure the transit time in terms of the modulation period. Measurements at different modulation frequencies permit the resolution of path length ambiguity. A high modulation frequency (3 GHz) was chosen because, for a given precision of phase measurement, the transit time can be measured more accurately at higher frequencies. Although most existing

instruments use information frequencies of the order of 10 MHz, it appears that the optimum frequencies for precise distance measurement may in fact lie in the UHF or microwave range (300-3000 MHz). This instrument, having a modulation wavelength of 10 cm, will measure the one-way distance to a precision of 1.5 mm if the modulation phase can be determined within 10^0 , a relatively easy task.

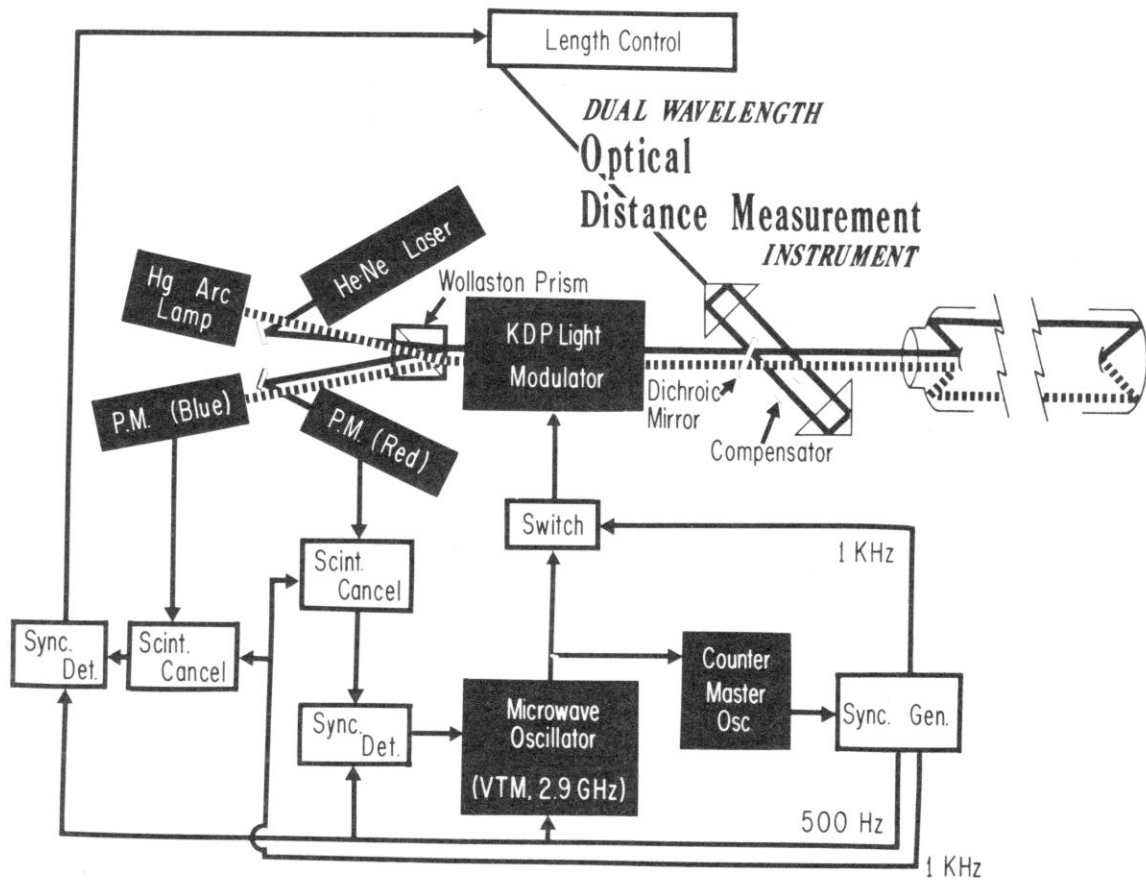
The arrangement for measuring the difference in optical path is very simple. The blue light is transmitted directly from the modulator to the telescope, but the red light is diverted by a dichroic mirror and two prism reflectors around an adjustable supplementary path. By adjusting the position of one of the reflectors to give simultaneous intensity maxima for both colors, the optical paths for red and blue are made equal, aside from an integral number of modulation wavelengths, and the difference in atmospheric optical path may be read out simply in terms of the distance the prism is moved from a reference position.

This instrument was first field tested during August 1966 over a 1.6-km path across Lake Hefner, near Oklahoma City. Although conditions were considerably less than optimum because of technical difficulties, the precision of the instrument in detecting optical path length changes for either wavelength was found to be about 0.03 ppm with an averaging time of 10 sec, and the standard error of corrected distance found from 177 measurements during a four-day period was slightly less than 1 ppm. Tests over a 5.3-km path between two hills north of Boulder were carried out in May 1967, using an instrument which had been rebuilt and improved. During these measurements, the normal rms fluctuations of 1-sec averages of apparent distance relative to the 30-sec moving average were found to be 3×10^{-9} of the total path, and a reproducibility of 0.3 ppm in corrected distance was found from 14 measurements over a period of two hours. Since then, the electronic and optical systems of the instrument have been extensively reworked to reduce a number of noise problems, and new measurements should be made soon. In particular, work is planned in the two-mile evacuable support pipe of the Stanford Linear Accelerator south of San Francisco, where measurements at various air densities can be made and the results used to determine the absolute accuracy of the correction method.

3. WATER VAPOR MEASUREMENT.

Meteorological measurements have traditionally been point measurements. In some cases, however, measurements integrated along a line or within a volume would be more useful, as in estimating the mass divergence of water vapor in studies of evaporation and of thunderstorm formation. Just as the dispersion of dry air makes possible the use of optical dispersion measurements for the determination of dry air density, so the much larger effect of water vapor on the microwave refractive index than on the optical makes possible the use of microwave-optical dispersion measurements for the determination of average water vapor density. A water vapor partial pressure of 10 mb at 15°C . increases the radio refractive index by 45 N-units (45 ppm in n) relative to that for the same total pressure of dry air. Hence a measurement of microwave transit time alone accurate to 1 ppm, in conjunction with adequate estimates of average pressure, average temperature, and true path length, gives the water vapor density to an accuracy of 2%. Suitable instruments for such measurements have been described in detail (GILMER and WATERS, 1967). In practice, uncertainties in average temperature limit the measurement accuracy to about 4% even on quite uniform paths only one mile long (BEAN and MCGAVIN, 1967).

This accuracy can be improved by adding a single-wavelength optical measurement to the microwave one. If the true path length is known, the optical measurement gives the average dry air density over the path. The average pressure can be



68823

Figure 3.1. Block diagram of the ESSA two-wavelengths, microwave-modulation-frequency distance measuring instrument.

determined satisfactorily from barometric measurements at the end points of the path, and hence the average temperature can be determined from the average density. With this source of error removed, the average water vapor density can be found to an accuracy of about 2.5% (if both measurements are accurate to 1 ppm) or about 0.5% (if both are accurate to 0.1 ppm) (BEAN and McGAVIN, 1967). The addition of a second optical wavelength does not improve the 0.5% figure, but does eliminate the need for independent knowledge of pressure and true path length (THOMPSON, 1968). Three-wavelength measurements have been reported (BEAN and McGAVIN, 1967), and a new two-wavelength microwave-optical instrument is under construction at ESSA by Bean, Earnshaw, Gilmer, and Owens.

4. ANGLE MEASUREMENT.

As early as 1942, TENGSTROM (1967) realized that the combination of atmospheric density gradients and atmospheric dispersion causes different wavelengths of light to be refracted by different amounts and that, if the resulting difference in angle of arrival were measured, it should be possible to determine the average vertical or horizontal gradient of refractive index and hence the total refraction angle for either wavelength. Thus the true direction to a light source could be found. For comparison with distance measurement, it is reasonable to say that an angle measurement which is accurate to 1 μ rad (1/5 sec of arc) has been made to 1 ppm.

Unfortunately, the precision required in the differential angle measurement is very high. Unlike distance measurement, the phase rather than the group refractive index is involved here. For a path length of 10 km, wavelengths of 6328 Å and 3660 Å, and a normal vertical gradient of refractive index, the difference between the true and apparent directions to the source for either wavelength is only about 30 sec of arc, and the difference between the angles of arrival for the two wavelengths is 0.9 sec (BEAN and DUTTON, 1966). The difference must therefore be measured to one part in 30, or 0.03 sec of arc, to determine the true direction to 1 sec (5 ppm). This cannot be done with a telescope or theodolite, and requires interferometry. It can easily be shown that for a double-slit interferometer having a slit spacing of 10 cm, a movement of the fringe pattern for 6328 Å by one fringe spacing corresponds to a change in angle of arrival of about 1 sec of arc. Hence the relative position of the patterns for the two wavelengths would have to be measured to about 1/30 fringe to give the corrected angle to 1 sec of arc. This may be possible with electronic scanning, but it would be a formidable task by eye. We conclude that the dispersion method can be of significant help in reducing the uncertainty in vertical angle measurements made from only one end of the line from several tens of seconds of arc to a few seconds. In horizontal angle measurement, however, for which the total refraction effect is normally only a few seconds of arc or less, little improvement can be expected.

One could increase the slit spacing to decrease the precision with which the relative fringe position must be measured, but it can be shown from the theory of optical propagation in Kolmogoroff turbulence (FRIED, 1967) that the rms fluctuation in angle of arrival increases almost as rapidly with slit spacing as does the sensitivity of the interferometer; consequently the improvement in signal-to-noise ratio is slight unless the detector tracks the fringes to first order. Moreover, for paths a few kilometers long close to the ground, it can be shown that the rms fluctuation in angle of arrival reaches one radian, causing a severe noise problem, at a slit spacing of only a few centimeters. There is some experimental indication, however, that the angle of arrival fluctuations do not in fact increase as rapidly with slit spacing as the theory predicts (BERTOLOTTI et al, 1968), and the situation may be more hopeful. Direct measurements of these fluctuations are being made by

Coulman of the National Standards Laboratory, C.S.I.R.O., Australia, by Tengstrom at the University of Uppsala in Sweden, and by Bouricius and Owens at ESSA, but no results have been reported yet.

5. CONCLUSION.

For measuring geodetic networks in which the sides are a few kilometers long, one-wavelength optical methods are capable of accuracies of a few ppm in distance, horizontal angle, and vertical angle differences, and of a few tens of ppm in absolute vertical angle when observations are made from one end of the line only. The two- and three-wavelength dispersion methods appear to make possible improvements of one and two orders of magnitude, respectively, in distance measurement, and to permit the determination of average water vapor density along a line to 0.5%. The dispersion method could also be applied to angle measurement, but this problem appears to be considerably more difficult. An accuracy of a few seconds of arc, and perhaps one second of arc, should be attainable. It is clear that the accuracy of distance measurements will soon surpass that of angle measurements by a considerable margin, and that trilateration will replace triangulation and mixed systems for work of the highest accuracy.

REFERENCES:

- JORDAN-EGGERT-KNEISSL
1966 Handbuch der Vermessungskunde, Band VI: Die Entfernungsmessung mit Elektro-Magnetischen Wellen und ihre Geodätische Anwendung.
K. Rinner and F. Benz, Eds., J.B. Metzlersche Verlagsbuchhandlung, Stuttgart.
- BENDER, P.L.
1967 Laser measurements of long distances. Proc. IEEE, 55, 1039-1045.
- INT.ASSN.
GEODESY
1965 Electromagnetic Distance Measurement. Proc. Int. Assn. Geodesy Symposium, Oxford, England, 1965. Pub. Hilger and Watts, London, 1967.
- INT. ASSN.
GEODESY
1967 Osterreichischen Zeitschrift für Vermessungswesen, Sonderheft 25, 1967. Proc. Int. Assn. Geodesy Symposium on Figure of the Earth and Refraction, Vienna, 1967.
- OWENS, J.C.
1968 The use of atmospheric dispersion in optical distance measurement, Bull. Geodesique, No. 89, 277-291.
- OWENS, J.C.
1967 Optical refractive index of air: dependence on pressure, temperature, and composition, Appl. Opt. Vol. 6, 51-59.
- THAYER, G.D.
1967 Atmospheric effects on multiple-frequency range measurements. ESSA Tech. Rept. IER 56-ITSA 53, U.S. Government Printing Office.
- BEAN, B.R. &
EMMANUEL, C.B.
1967 Application of radio and optical path length measurements to studies of low level turbulence. Proc. Joint Technical Exchange Conference, Monterey, Calif., 1967.

- McQUISTAN, G.W. 1968 Electromagnetic distance measuring with two wavelengths, Technical Memorandum PAD 262, Dept. of Supply, Australian Defence Scientific Service, Weapons Research Establishment. (see also G.W. McQuistan, Electromagnetic distance measuring with two wavelengths - atmospheric limitations, Paper No. 4 in the present volume.)
- FOWLER, R.A. & CASTELLANO, V. 1966 Geodetic laser survey system (GLASS) - an application to earthquake prediction, Trans. Am. Geophys. Union, Vol. 47, 166-167.
- THOMPSON JR., M.C. & WOOD, L.E. 1965 The use of atmospheric dispersion for refraction correction of optical distance measurements, IAG EDM Symposium, Oxford 1965, pp 165-171.
- SULLIVAN, J.F. 1965 Final report on line integral refractometer. Report MTP-19, Mitre Corporation, Lexington, Massachusetts.
- EARNSHAW, K.B. & OWENS, J.C. 1967 A dual wavelength optical distance measuring instrument which corrects for air density. IEEE J. Quantum Electronics, QE-3, 544-550.
- GILMER, R.O. & WATERS, D.M. 1967 A solid-state system for measurement of integrated refractive index. Tech. Rept. IER-40/ITSA-40, U.S. Government Printing Office.
- BEAN, B.R. & MCGAVIN, R.E. 1967 Electromagnetic phase variability as a measure of water vapor and temperature variations over extended paths. Proc. AGARD-ERPC Symposium on Phase and Frequency Instability in Electromagnetic Wave Propagation, Ankara, Turkey, 1967.
- THOMPSON JR., M.C. 1968 Space averages of air and water vapor densities by dispersion for refractive correction of electromagnetic range measurements. J. Geophys. Res. Vol. 73, 3097-3102.
- TENGSTROM, E. 1967 Elimination of refraction at vertical angle measurements, using lasers of different wavelengths. IAG Symposium, Vienna, 1967, 292-303.
- BEAN, B.R. & DUTTON, E.J. 1966 Radio Meteorology. NBS Monograph 92, U.S. Government Printing Office, Washington.
- FRIED, D.L. 1967 Optical heterodyne detection of an atmospherically distorted signal wave front. Proc. IEEE, Vol. 55, 57-67.
- BERTOLOTTI, M. CARNEVALE, M. L. MUZZI, & SETTE, D. 1968 Interferometric study of phase fluctuations of a laser beam through the turbulent atmosphere. Appl. Opt. Vol. 7, 2246-2251.

ELECTROMAGNETIC DISTANCE MEASURING WITH TWO WAVELENGTHS
- ATMOSPHERIC LIMITATIONS.

G.W. McQuistan

SUMMARY. An assessment is made of the accuracies in the measurement of distance by Electromagnetic Distance Measuring Systems operating in the lower atmosphere. The accuracy of a double wavelength system is at least an order better than that of a single wavelength system if certain parameters (phase or time) are measurable with sufficient accuracy.

1. INTRODUCTION.

Electromagnetic distance measurement is widely used and commercial systems are available using both microwave and optical carriers. A significant improvement in accuracy is available if two optical carriers are used and the advent of lasers has meant that dual wavelength systems can be operated over large distances in daylight.

In this paper a comparison is made of the atmospheric limitations of systems using one and two wavelengths.

2. THE VELOCITY OF LIGHT.

The vacuum velocity of light will be assumed known and constant (c). In a vacuum therefore, the time for light to travel from A to B, a distance L , is given by

$$t_{\text{vac}} = L/c \quad (1)$$

In a non-dispersive medium which has refractive index n_1 at a point within AB, the time for light to travel from A to B is

$$t_{\text{ND}} = \left(\frac{1}{c}\right) \int_0^L n_1 d_1 \quad (2)$$

The atmosphere is non-dispersive (in general) at radio frequencies and Eq. (2) is therefore applicable to Tellurometers.

At optical wavelengths the atmosphere is dispersive and the time of travel of light is therefore

$$t_D = \left(\frac{1}{c}\right) \int_0^L n_1^G dl \quad (3)$$

where n_1^G is the group refractive index, σ is the vacuum wavenumber (in micron^{-1}), and $n_1^G = n_1 + \sigma \, dn_1/d\sigma$.

3. THE DISTANCE MEASURING PROBLEM.

Electromagnetic distance measuring is performed either by measuring the time of propagation of the radiation or by phase comparison of a transmitted and received modulation. In this paper a system of time measurement is assumed but the same considerations apply to the more generally used phase comparison system.

To measure distance by timing the propagation of electromagnetic waves involves the evaluation of the right hand sides of Eqs. (2) or (3) depending on whether microwave or optical wavelengths are used. Both equations present the same difficulty - the evaluation of the integral, $\int n_1 dl$, or using the refractivity, the integral $\int (n-1)dl$; since

$$\begin{aligned} \int_0^L n_1 dl &= \int_0^L (1 + n_1 - 1) dl \\ &= L + \int_0^L (n_1 - 1) dl \end{aligned}$$

A first approximation can be derived by assuming n_1 is constant and evaluating it from meteorological data. By making many measurements along the path improved "average" values of n_1 can be obtained but errors obtained by this method are more than 1 part in 10^6 .

Variations in refractive index result from atmospheric density changes. (The composition, apart from water vapour, is assumed constant.) The density is specified by the temperature, total pressure and partial pressure of water vapour. In general, the atmosphere is subject to variations in density over a wide range of scales from the large weather patterns (1000 miles) to the microscales of turbulence (millimetres). Consequently a sophisticated system of instruments is required to obtain the mean refractive index to the required accuracy.

Owens gives the following formulae for the group refractivity of the atmosphere (OWENS, 1967, Eqs. 42, 30, 31).

$$\begin{aligned} (n^G - 1) \times 10^8 &= [2371.34 + 683939.7(130 + \sigma^2)/(130 - \sigma^2)^2 \\ &\quad + 4547.3(38.9 + \sigma^2)/(38.9 - \sigma^2)^2] D_S \\ &\quad + [6487.31 - 174.174 \sigma^2 - 3.55750\sigma^4 + 0.61957\sigma^6] D_W \end{aligned} \quad (4)$$

where σ is the vacuum wavenumber (microns^{-1})

$$\text{and } D_S = \frac{P_S}{T} [1 + P_S(57.9 \times 10^{-8} - 9.3250 \times 10^{-4}/T + 0.25844/T^2)] \quad (5)$$

$$\text{and } D_W = \frac{P_W}{T} \{1 + P_W [1 + (3.7 \times 10^{-4})P_W] [-2.37321 \times 10^{-3} + 2.23366/T - 710.792/T^2 + 7.75141 \times 10^4/T^3]\} \quad (6)$$

where P_S is the partial pressure of the dry air (millibars),

P_W is the partial pressure of water vapour (millibars), and

T is the temperature ($^{\circ}\text{K}$).

Formula (4) will be used below in the form

$$(n^G - 1) \times 10^8 = A_{\sigma} D_S + B_{\sigma} D_W \quad (7)$$

4. SINGLE WAVELENGTH METHOD.

Although the meteorological factors have different weights, depending upon the wavenumber of the radiation, Eqs. (4) or (7) express the correct relationship for all wavenumbers including dispersive and non-dispersive cases.

Therefore substituting Eq. (7) in (3) gives:

$$t = \left(\frac{1}{c}\right) \int_0^L dl + 10^{-8} \left(\frac{1}{c}\right) \int_0^L (A_{\sigma} D_S + B_{\sigma} D_W) dl \quad (8)$$

The first term is L/c . Re-arranging Eq. (8) and solving for L :

$$L = ct - 10^{-8} \left[A_{\sigma} \int_0^L D_S dl + B_{\sigma} \int_0^L D_W dl \right] \quad (9)$$

If by averaging we obtain mean values of D_S and D_W , say \bar{D}_S and \bar{D}_W , Eq. (9) reduces to

$$L = ct [1 - 10^{-8} (A_{\sigma} \bar{D}_S + B_{\sigma} \bar{D}_W)] \quad (10)$$

Assuming the averaging process has involved errors due to the practical impossibility of measuring temperature pressure and water vapour pressure at every point along L then an error dL will result in the distance measurement. By taking the complete differential of (10)

$$dL/L = -10^{-8} \left\{ A_{\sigma} \frac{\partial D_S}{\partial T} dT + A_{\sigma} \frac{\partial D_S}{\partial P_S} dP_S + B_{\sigma} \frac{\partial D_W}{\partial P_W} dP_W + B_{\sigma} \frac{\partial D_W}{\partial T} dT \right\} \quad (11)$$

where $\partial D_S/\partial T$ is the partial derivative of D_S with respect to T , and dT is the error in averaging T , etc. This relationship (11) will be used below in comparison with a similar one derived for the dual wavelength system to show that for the same errors in averaging (i.e. the same dT , dP_S and dP_W) the relative error in distance measurement (dL/L) is smaller when two wavelengths are used.

5. ADDITIONAL INFORMATION USING TWO WAVELENGTHS.

Before proceeding to analyse the dual wavelength system it is necessary to see what additional information is gained.

Consider the two equations similar to (9) that can be written down for the two wavenumbers σ_1 and σ_2 .

$$L = ct_1 - 10^{-8} \left[A_{\sigma_1} \int_0^L D_S dl + B_{\sigma_1} \int_0^L D_W dl \right] \quad (12a)$$

$$L = ct_2 - 10^{-8} \left[A_{\sigma_2} \int_0^L D_S dl + B_{\sigma_2} \int_0^L D_W dl \right] \quad (12b)$$

Firstly it must be pointed out that to take the difference of these equations, to apply averaging to D_S and D_W and to then solve for L is not acceptable as L is then proportional to $t_1 - t_2$, and dL/L is proportional to $d(t_1 - t_2)/(t_1 - t_2)$. Unless a system is available which can measure $d(t_1 - t_2)/(t_1 - t_2)$ better than dt_1/t_1 , (see Section 7) this procedure will not be the most accurate. Furthermore in the general situation where the refractive index varies, L is not proportional to $t_1 - t_2$.

Returning to Eqs. (12a) and (12b). In these two equations there are three unknowns: L , $\int_0^L D_S dl$ and $\int_0^L D_W dl$. Any of these may be eliminated. Removing L has already been discussed as an indirect way of finding L , but it does give some information about the problem integrals.

Eliminating L

$$c(t_1 - t_2) = 10^{-8} \left[(A_{\sigma_1} - A_{\sigma_2}) \int_0^L D_S dl + (B_{\sigma_1} - B_{\sigma_2}) \int_0^L D_W dl \right] \quad (13)$$

The right hand side of this equation depends only on the difference in refractive index which we might reasonably assume does not depend so strongly on the averaging errors as the refractive indices themselves.

Furthermore if in equations (12) the L on the left hand side can be kept isolated for evaluation it would be more accurately determined as the first term on the right hand side ct_1 , is large and the second one, where the errors originate, is small.

Therefore multiplying the second term of (12a) by the left hand side of (13) and dividing by the right hand side of (13) the result is

$$L = ct_1 - \frac{(ct_1 - ct_2) \left[A_{\sigma_1} \int_0^L D_S dl + B_{\sigma_1} \int_0^L D_W dl \right]}{\left[(A_{\sigma_1} - A_{\sigma_2}) \int_0^L D_S dl + (B_{\sigma_1} - B_{\sigma_2}) \int_0^L D_W dl \right]} \quad (14)$$

If, as was done for the single wave case, average values are given to D_S and D_W Eq. (14) becomes

$$L = ct_1 - \frac{(A_{\sigma_1} \bar{D}_S + B_{\sigma_1} \bar{D}_W) (ct_1 - ct_2)}{[(A_{\sigma_1} - A_{\sigma_2}) \bar{D}_S + (B_{\sigma_1} - B_{\sigma_2}) \bar{D}_W]} \quad (15)$$

On the right hand side L has been eliminated.

It now remains to prove that this provides smaller errors in the determination of L than Eq. (10).

Taking the complete differential of Eq. (15)

$$\frac{dL}{L} = \frac{10^{-8} (A_{\sigma_2} B_{\sigma_1} - A_{\sigma_1} B_{\sigma_2})}{(A_{\sigma_1} - A_{\sigma_2}) \bar{D}_S + (B_{\sigma_1} - B_{\sigma_2}) \bar{D}_W} \left[\left(\frac{\partial D_S}{\partial T} dT + \frac{\partial D_S}{\partial P_S} dP_S \right) \bar{D}_W - \left(\frac{\partial D_W}{\partial P_W} dP_W + \frac{\partial D_W}{\partial T} dT \right) \bar{D}_S \right] \quad (16)$$

To evaluate the coefficient of this expression $K_{12} = \frac{(A_{\sigma_2} B_{\sigma_1} - A_{\sigma_1} B_{\sigma_2})}{(A_{\sigma_1} - A_{\sigma_2}) \bar{D}_S + (B_{\sigma_1} - B_{\sigma_2}) \bar{D}_W}$ /

$[(A_{\sigma_1} - A_{\sigma_2}) \bar{D}_S + (B_{\sigma_1} - B_{\sigma_2}) \bar{D}_W]$ the values of A and B were calculated from Eq. (4).

These are given below in Table I.

TABLE I. VALUES OF THE COEFFICIENTS A_{σ} AND B_{σ}

Wavenumber (microns ⁻¹)	0.5	1	1.5	2	2.5	3
Wavelength (microns)	2	1	0.67	0.5	0.4	0.33
A_{σ}	7.78x10 ³	7.88x10 ³	8.09x10 ³	8.30x10 ³	8.65x10 ³	9.11x10 ³
B_{σ}	6.53x10 ³	6.66x10 ³	6.87x10 ³	7.17x10 ³	7.59x10 ³	8.22x10 ³

Values of K_{12} have been calculated in an investigation of choice of optimum wavenumbers. These are given in Appendix I and from there it will be seen that they are all of the order of 10^3 which will be taken as the value for comparison purposes.

Thus from Eq. (16)

$$\frac{dL}{L} = 10^{-5} \left(D_W \frac{\partial D_S}{\partial T} dT + D_W \frac{\partial D_S}{\partial P_S} dP_S - D_S \frac{\partial D_W}{\partial P_W} dP_W - D_S \frac{\partial D_W}{\partial T} dT \right) \quad (17)$$

This must be compared with Eq. (11) for the single wavelength case, repeated here

$$\frac{dL}{L} = 10^{-8} \left(A_{\sigma} \frac{\partial D_S}{\partial T} dT + A_{\sigma} \frac{\partial D_S}{\partial P_S} dP_S + B_{\sigma} \frac{\partial D_W}{\partial P_W} dP_W + B_{\sigma} \frac{\partial D_W}{\partial T} dT \right) \quad (18)$$

As P_W , the partial pressure of the water vapour content, varies over the range 0 to 10^2 mb and P_S , the partial pressure of the dry air is always about 10^3 mb, from Eqs. (5) and (6), D_W varies from 0 to 3.5×10^{-1} and D_S is always about 3.5

A comparison of the coefficients in Eqs. (17) and (18) shows that those of the dual wavelength system (17) are always less than the single wavelength case (18). A quantitative comparison is given in the following section.

6. ATMOSPHERIC PARAMETERS AND THE ERRORS IN DISTANCE MEASUREMENT.

The total atmospheric pressure varies only by a few percent at sea level and a value of 1000 mb will be assumed.

i.e. $P_S + P_W = 1\ 000\ \text{mb}$

The temperature range considered will be 273.16 to 318.16°K

i.e. 0 to 113°F.

The partial pressure of water vapour varies from zero to a maximum value dependent on the temperature. This maximum value, which is the partial pressure for 100% humidity, is given in Table II.

TABLE II. PARTIAL PRESSURE OF WATER VAPOUR FOR 100% HUMIDITY AT VARIOUS TEMPERATURES

Temperature (°K)	273.16	288.16	303.16	318.16
Temperature (°C)	0	15	30	45
Partial pressure for 100% humidity (mb)	6.13	17.07	42.28	95.54

The various partial derivatives can be calculated from Eqs. (5) and (6) for the range of parameters.

$\frac{\partial D_S}{\partial T} = \frac{-P_S}{T^2}$ approximately $-1.2 \times 10^{-2}/^\circ\text{K}$

$\frac{\partial D_W}{\partial T} = \frac{-P_W}{T^2}$ varies from zero ($P_W=0$) to $-9.5 \times 10^{-4}/^\circ\text{K}$ ($P_W=95.54\ \text{mb}$)

$\frac{\partial D_S}{\partial P_S} = \frac{1}{T}$
 $\frac{\partial D_W}{\partial P_W} = \frac{1}{T}$ } approximately $3.5 \times 10^{-3}/\text{mb}$

Consider now a typical atmosphere and the errors produced firstly in the single wavelength system. Let $P_S + P_W = 1\ 000\ \text{mb}$, $T = 288.16^\circ\text{K}$ and 50% relative humidity (i.e. $P_W = 8.53\ \text{mb}$).

Then from Eq. (18) for $\sigma = 2\mu^{-1}$ (5 000Å)

$$\frac{dL}{L} = -10^{-6} dT + 2.8 \times 10^{-7} dP_S + 2.5 \times 10^{-7} dP_W - 7.0 \times 10^{-9} dT_W \quad (19)$$

Now dT , dP_S , dP_W (dT_W is kept separate as its coefficient depends on P_W but it is equal to dT) are the errors in estimating the average T , P_S and P_W over the whole distance and include measuring errors. In a typical atmosphere, observations at one position show r.m.s. variations in these quantities over a short period of time (minutes) as follows

$$\Delta T \approx 1^\circ K$$

$$\Delta(P_S + P_W) < 10^{-2} \text{ mb}$$

$$\Delta P_W < 4 \times 10^{-2} P_W \text{ (in this case 0.34 mb)}$$

If it is assumed that the averaging errors are equal to these r.m.s. values it becomes obvious which are the most important parameters as

$$\frac{dL}{L} = \underbrace{-10^{-6}}_{(T)} + \underbrace{2.8 \times 10^{-9}}_{(P_S)} + \underbrace{8.3 \times 10^{-8}}_{(P_W)} - \underbrace{7 \times 10^{-9}}_{(T)} \quad (20)$$

It must be noted that as $P_S + P_W$ is not greatly variable the terms P_S and P_W will be of opposite sign.

Therefore, when using only one wavelength, temperature is the most important parameter to establish and it is reasonable that accuracies of 1 part in 10^6 are seldom attained.

Applying the Dual Wavelength equation to this same situation

$$\frac{dL}{L} = -3.5 \times 10^{-9} dT + 10^{-9} dP_S - 1.2 \times 10^{-7} dP_W - 3.5 \times 10^{-9} dT \quad (21)$$

and when the r.m.s. values are applied

$$\frac{dL}{L} = \underbrace{-3.5 \times 10^{-9}}_{(T)} + \underbrace{10^{-11}}_{(P_S)} - \underbrace{4.1 \times 10^{-8}}_{(P_W)} - \underbrace{3.5 \times 10^{-9}}_{(T)} \quad (22)$$

In this typical situation it may be expected that errors of about 5 part in 10^8 could be obtained. In Table III dL/L is given for a range of situations covering those found in the atmosphere.

TABLE III. RELATIVE ERROR IN DISTANCE (dL/L) FOR SINGLE (S) AND DUAL (D) WAVELENGTH SYSTEMS

Temp °K	273.16		288.16		303.16		318.16	
Temp °C	0		15		30		45	
Relative Humidity	S	D	S	D	S	D	S	D
	0	1.00x10 ⁻⁶	0	1.00x10 ⁻⁶	0	1.00x10 ⁻⁶	0	1.00x10 ⁻⁶
50%	1.03x10 ⁻⁶	2.0x10 ⁻⁸	1.09x10 ⁻⁶	4.8x10 ⁻⁸	1.21x10 ⁻⁶	1.04x10 ⁻⁷	1.48x10 ⁻⁶	2.08x10 ⁻⁷
100%	1.06x10 ⁻⁶	4.0x10 ⁻⁸	1.17x10 ⁻⁶	8.7x10 ⁻⁸	1.42x10 ⁻⁶	2.10x10 ⁻⁷	1.95x10 ⁻⁶	3.94x10 ⁻⁷

Assumed averaging errors $dT = 1^{\circ}K$, $dP_S = 10^{-2}$ mb, $dP_W = 4 \times 10^{-2} P_W$

$P_S + P_W = 1\ 000$ mb

The Dual Wavelength System is therefore more accurate than the single optical wavelength system and it is two orders better at low humidity.

7. TIMING REQUIREMENTS.

So far, only the atmospheric limitations have been considered and it is now necessary to see what accuracy is required from the time measurements.

The basic distance determining Eq. (15) may be written in the form

$$L = ct_1 - \frac{(n_1 - 1)}{(n_1 - n_2)} c (t_1 - t_2) \tag{23}$$

where n_1 and n_2 are the average refractive indices. In the above sections, the error in L due to errors in n_1 and n_2 has been considered and will now be subscripted as $(dL/L)_n$.

Taking the complete differential of Eq. (23), this time including the time factors t_1 and $t_1 - t_2$ as separate variables

$$\frac{dL}{L} = \left(\frac{dL}{L}\right)_n + \frac{dt_1}{t_1} + \frac{(n_1 - 1)d(t_1 - t_2)}{t_1 - t_2} \tag{24}$$

using the relationship

$$L/c = (t_1 - t_2)/(n_1 - n_2) \tag{25}$$

The data of table III indicates that under most normal conditions an accuracy of 1 part in 10^{+7} is attainable and that the timing accuracy should be, therefore, as good as this. Therefore dt_1/t_1 should be $< 10^{-7}$

$$\tag{26}$$

and $d(t_1 - t_2)/(t_1 - t_2)$ should be $< 10^{-7}/(n_1 - 1) = 3 \times 10^{-4}$

$$\tag{27}$$

This may also be considered by using the relationship between $t_1 - t_2$ and t_1 namely

$$t_1 - t_2 = \frac{(n_1 - n_2)}{n_1} t_1$$

Substituting this in Eq. (27)

$$d(t_1 - t_2)/t_1 \text{ should be } < \frac{(n_1 - n_2)}{n_1(n_1 - 1)} 10^{-7} \approx 7 \times 10^{-9}$$

Therefore the requirement of Eq. (26) does not include that of Eq. (27): rather the latter is a separate requirement.

For example consider the timing accuracies required to measure a distance of 15 km (double pass)

$$\begin{aligned} t_1 &= 10^{-4} \text{s} & \text{therefore} & \quad dt_1 < 10^{-11} \text{s} \\ t_1 - t_2 &= 2 \times 10^{-5} t_1 & & \quad (\sigma_1 = 3, \sigma_2 = 1) \\ &= 2 \times 10^{-9} \text{s} \end{aligned}$$

$$\text{Therefore } d(t_1 - t_2) < 6 \times 10^{-13} \text{s.}$$

While dt_1/t_1 is independent of the wavelengths used $d(t_1 - t_2)/(t_1 - t_2)$ can be reduced by making $(t_1 - t_2)$ large, that is by choosing n_1 in the blue region and n_2 in the red or infra-red.

The purpose of this paper is not to discuss how this accuracy may be achieved but to establish the theoretical limiting factors. However it does seem likely that such accuracies will be achievable and although the assumption has been implied throughout that the system is one of the pulsed or phase measuring type, these are not the only ones (EARNSHAW and OWENS, 1967) and the above analysis is applicable whether times or distances are measured.

Two further points must be made concerning accuracy. Firstly, the velocity of light has been assumed known and although it is known only to about 1 part in 10^6 it is used here only as a convenience in transferring from the standard distance measurements (i.e. wavelength).

Secondly, the coefficients in Eq. (4) have been assumed without question and as these have been differenced some consideration of this point is necessary. Owens has deduced these particular values and obtains agreement with other formulae to better than 1 part in 10^6 . (OWENS, 1967) Some further investigation seems necessary on this point, particularly in regard to the narrow bands that the lasers use.

8. GENERAL REMARKS.

The method of determining distance described above is not the only one that follows from the use of two wavelengths but it is considered the best. The basic

Eqs. are (12a) and (12b) and these may be regarded as simultaneous equations in three unknowns (namely L , $\int_0^L D_S dl$ and $\int_0^L D_W dl$). The method above shows how by averaging the second two unknowns the first can be determined with high accuracy. However, it is theoretically possible to completely eliminate any of these unknown integrals, but from a practical point of distance measurement this is generally no advantage.

Having used two wavelengths to help in measuring the atmospheric conditions the question arises, why stop at only two? Quantitatively this question hasn't been investigated in this work, but it is obvious that adding an extra wavelength would provide another equation similar to (12a) and (12b) giving three equations in three unknowns. The solution can then be expressed by the matrix equation

$$\begin{pmatrix} c/L \\ L \\ \int_0^L D_S dl/L \\ L \\ \int_0^L D_W dl/L \end{pmatrix} = \begin{pmatrix} t_1 & -A_{\sigma_1} & -B_{\sigma_1} \\ t_2 & -A_{\sigma_2} & -B_{\sigma_2} \\ t_3 & -A_{\sigma_3} & -B_{\sigma_3} \end{pmatrix}^{-1} \begin{pmatrix} 1 \\ 1 \\ 1 \end{pmatrix}$$

The three quantities on the left hand side are of great interest not only for this application to distance measuring but also for the information they provide about the atmosphere.

9. CONCLUSION.

The relative error in a single wavelength electromagnetic distance measuring system is limited by the atmosphere to about 1 part in 10^6 . Using two wavelengths the same atmospheric limitation enables relative errors of about 1 part in 10^7 to be achieved. For the dual wavelength system time of propagation must be determined to 1 part in 10^7 and the time difference to 3 parts in 10^4 . By using three wavelengths, the distance measurement can be made independent of the atmospheric limitation and can also provide important information on the atmosphere itself.

REFERENCES.

OWENS, J.C. Optical Refractive Index of Air: Dependence on Pressure, Temperature and Composition. Applied Optics, Vol.6, No. 1. 1967

EARNSHAW, K.B. and A Dual Wavelength Instrument which Measures Air Density. OWENS, J.C. IEEE Journal of Quantum Electronics, p. 257. 1967

GENERAL REFERENCES.

- WHITTEN, C.A. and SCHMID, E. (Editors) International Symposium on Electronic Distance Measuring Techniques. Journal of Geophysical Research, Vol. 65 No. 2, pp. 385-528.
1960
- DENISON, E.W. Report of Special Study Group No. 19: Electromagnetic Distance Measurement, 1963-1967. Int. Assn. Geodesy.
1967
- BENDER, P.L. Laser Measurements of Long Distances. Proceedings of the IEEE, Vol. 55, No. 6, p. 1039.
1967
- BAIRD, R.C. R.F. Measurements of the Speed of Light. Proceedings of the IEEE, Vol. 55, No. 6, p. 1032.
1967
- INT. ASSN. GEODESY International Symposium on Electromagnetic Distance Measurement. SSG 19, I.A.G. Oxford 1965. Pub. Hilger and Watts, 1967.
1965

APPENDIX 1.

OPTIMUM WAVENUMBERS FOR DUAL WAVELENGTH DISTANCE MEASURING
DETERMINED BY ATMOSPHERIC PARAMETERS

The errors introduced into the distance measurement in the Dual Wavelength System by the atmosphere are all proportional to a factor K where

$$K = \frac{A_{\sigma_2} B_{\sigma_1} - A_{\sigma_1} B_{\sigma_2}}{(A_{\sigma_1} - A_{\sigma_2})D_S + (B_{\sigma_1} - B_{\sigma_2})D_W} \quad (\text{See Eq. (16)})$$

The terms A_{σ} and B_{σ} are determined by Eqs. (4) and (7) and D_S and D_W are given by Eqs. (5) and (6).

The above factor has been determined for various combinations of wavenumbers and atmospheric conditions and its values are given in the following tables. The values are given in terms of mean wave number and half wavenumber separation.

$$\text{Mean Wavenumber } \bar{\sigma} = (\sigma_1 + \sigma_2)/2$$

$$\text{Half Wavenumber separation } \Delta\sigma = (\sigma_1 - \sigma_2)/2$$

FACTOR K FOR $P_S = 1\ 000\ \text{mb}$, $P_W = 0$, $T = 288.16^\circ\text{K}$

$\Delta\sigma \backslash \bar{\sigma}$	$0.5\ \mu^{-1}$	$1.0\ \mu^{-1}$	$1.5\ \mu^{-1}$	$2.0\ \mu^{-1}$	$2.5\ \mu^{-1}$	$3.0\ \mu^{-1}$
$0.01\ \mu^{-1}$	1.07×10^3	0.940×10^3	0.805×10^3	0.772×10^3	0.954×10^3	1.45×10^3
$0.1\ \mu^{-1}$	1.07×10^3	0.936×10^3	0.805×10^3	0.776×10^3	0.960×10^3	1.45×10^3
$0.5\ \mu^{-1}$	-	0.914×10^3	0.816×10^3	0.826×10^3	1.05×10^3	-
$1.0\ \mu^{-1}$	-	0.873×10^3	0.904×10^3	1.00×10^3	-	-

FACTOR K FOR $P_S = 990\ \text{mb}$, $P_W = 10\ \text{mb}$, $T = 288.16^\circ\text{K}$

$\Delta\sigma \backslash \bar{\sigma}$	$0.5\ \mu^{-1}$	$1.0\ \mu^{-1}$	$1.5\ \mu^{-1}$	$2.0\ \mu^{-1}$	$2.5\ \mu^{-1}$	$3.0\ \mu^{-1}$
$0.01\ \mu^{-1}$	1.06×10^3	0.934×10^3	0.805×10^3	0.773×10^3	0.951×10^3	1.44×10^3
$0.1\ \mu^{-1}$	1.06×10^3	0.933×10^3	0.805×10^3	0.775×10^3	0.956×10^3	1.45×10^3
$0.5\ \mu^{-1}$	-	0.913×10^3	0.816×10^3	0.826×10^3	1.05×10^3	-
$1.0\ \mu^{-1}$	-	0.871×10^3	0.903×10^3	1.00×10^3	-	-

FACTOR K FOR $P_S = 900$ mb, $P_W = 100$ mb, $T = 288.16^\circ\text{K}$

$\Delta\sigma$	$0.5 \mu^{-1}$	$1.0 \mu^{-1}$	$1.5 \mu^{-1}$	$2.0 \mu^{-1}$	$2.5 \mu^{-1}$	$3.0 \mu^{-1}$
$0.01 \mu^{-1}$	1.03×10^3	0.913×10^3	0.790×10^3	0.759×10^3	0.927×10^3	1.38×10^3
$0.1 \mu^{-1}$	1.03×10^3	0.912×10^3	0.791×10^3	0.761×10^3	0.931×10^3	1.38×10^3
$0.5 \mu^{-1}$	-	0.893×10^3	0.802×10^3	0.811×10^3	1.02×10^3	-
$1.0 \mu^{-1}$	-	0.854×10^3	0.885×10^3	0.976×10^3	-	-

It is evident from the figures of these tables that as far as errors arising in the atmosphere are concerned, the choice of wavenumbers is hardly significant.

DISCUSSION: PAPERS 3 and 4.

Chairman: Mr. L.A. Gale

McQUISTAN: Atmospheric dispersion.

OWENS: Dual wavelength measurements.

ANGUS-LEPPAN: My measurements and investigations show a great dependence on height above the surface, particularly in the lowest layers above the surface. Has Owens found this dependence on height?

OWENS: We have not yet made measures of distance as a function of height above the surface, so we have no direct data on this question. We do know that the scintillation of light is a function of the height above the ground.

ROLF: Have you measured distance as a function of the time of day?

OWENS: Yes, but no correlation was seen. Perhaps the accuracy attained was not sufficient to reveal a statistically significant correlation. There was no obvious diurnal variation.

GALE: Experience in Canada shows no appreciable difference between the accuracy of results of day or night observations.

MACLEAN: What type of read-out does your equipment provide?

OWENS: Our equipment is specialised and for scientific measurements. It has not been developed to the stage where the read-out is in the most convenient form. It consists essentially of frequency counters, and the distance is computed from these readings.

POWELL: Is the velocity of light known sufficiently precisely for your measurements?

OWENS: This has been frequently quoted as a difficulty, but in fact an incorrect velocity has no measurable consequences. Provided c is known to 1 part per million, the effect is a scale factor, present in all e.d.m.'s, but which cannot be detected because we are unable to tape to better than 1 ppm. This refers to c in vacuo. Whether the formula for its value under atmospheric conditions is accurate, is a different question, and this is why we are to make measurements with our apparatus in a long evacuated pipe.

LEPPERT: What time of day or night gives optimum results with e.d.m?

OWENS: Our best results occur fairly early in the morning before sunrise or otherwise just after sunset. At night odd situations occur, and in daytime, turbulence causes strong scintillation.

ANGUS-LEPPAN: Owens' conclusions are explained by temperature conditions and scintillation, but there is a further reason for preferring early morning or evening observations. At these times the temperature gradient is very small, the lower layers being nearly isothermal. On a line with varying height above the surface, temperatures measured at the ends are more likely to be representative of the whole line.